Inorganic Chemistry

Article

pubs.acs.org/IC

Unexpected NO Transfer Reaction between *trans*-$[Ru^{II}(NO^+)(NH_3)_4(L)]^{3+}$ and Fe(III) Species: Observation of a Heterobimetallic NO-Bridged Intermediate

Gustavo Metzker,[†] Pietro P. Lopes,[†,‡] Augusto C. H. da Silva,[†] Sebastiao C. da Silva,[§] and Douglas W. Franco*,[†]

[†]Instituto de Química de São Carlos, Universidade de São Paulo, Avenida Trab. São-Carlense 400, São Carlos, SP, Brazil

[‡]Argonne National Laboratory, 9700 S Cass Avenue, Lemont, Illinois, United States

[§]Universidade Federal de Mato Grosso, Avenida Fernando Corrêa da Costa 2367, Cuiaba, MS, Brazil

Supporting Information

ABSTRACT: The reaction between *trans*-$[Ru^{II}(NO^+)(NH_3)_4(L)]^{3+}$, L = ImN, IsN, Nic, $P(OMe)_3$, $P(OEt)_3$, and $P(OH)(OEt)_2$, and the Fe(III) species $[Fe^{III}(TPPS)]$, metmyoglobin, and hemoglobin was monitored by UV−vis, EPR, and electrochemical techniques (DPV, CV). No reaction was observed when L = ImN, IsN, Nic, and $P(OH)(OEt)_2$. However, when L = $P(OMe)_3$ and $P(OEt)_3$, the reaction was quantitative and the products were *trans*-$[Ru^{III}(H_2O)(NH_3)_4(P(OR)_3)]^{3+}$ and $[Fe^{II}(NO^+)]$ species. Reaction kinetics data and DFT calculations suggest a two-step reaction mechanism with the initial formation of a bridged [Ru−(μNO)−Fe] intermediate, which was confirmed through electrochemical techniques ($E^{0\prime}$ = −0.47 V vs NHE). The calculated specific rate constant values for the reaction were in the ranges k_1 = 1.1 to 7.7 L mol^{-1} s^{-1} and $k_2 = 2.4 \times 10^{-3}$ to 11.4×10^{-3} s^{-1} for L = $P(OMe)_3$ and $P(OEt)_3$. The oxidation of the ruthenium center (Ru(II) to Ru(III)) containing the nitrosonium ligand suggests that NO can act as an electron transfer bridge between the two metal centers.

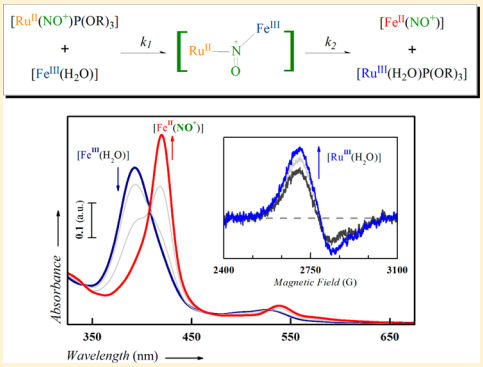

INTRODUCTION

Ruthenium nitrosyl complexes, *trans*-$[Ru^{II}(NO^+)(NH_3)_4(L)](X)_n$, are able to deliver nitric oxide (NO) or nitroxyl (HNO), *in vitro* and *in vivo*, after one- or two-electron reductions,[1−8] which are the key steps for the biological action of this class of compounds. Iron-containing proteins,[9] such as soluble guanylyl cyclase,[10] and thiol proteins[11] are the probable targets of these nitrogen oxides and result in various physiological effects.[12] Nitrosylation reactions with metalloproteins are important in nitrogen oxide biology and can occur via NO transfer between two metal centers. There are two proposed different pathways for this reaction (eqs 1/2 and eqs 3/4):[13−19]

$$[M(NO)]^n \rightleftharpoons [M]^n + NO \quad (1)$$

$$[M]^m + NO \rightleftharpoons [M(NO)]^m \quad (2)$$

$$[M(NO)]^n + [M]^m \rightleftharpoons [M(\mu\text{-}NO)M]^{n+m} \quad (3)$$

$$[M(NO)M]^{n+m} \rightleftharpoons [M(NO)]^m + [M]^n \quad (4)$$

In both mechanisms, there is no electron transfer between the two metal centers during the reaction. Also, NO instead of nitrosonium (NO^+) is involved in the reactions. Kinetics, DFT calculations, and binuclear identification data involving this type of reaction are scarce.

Metmyoglobin is used as a spectrophotometric probe to detect nitroxyl formation owing to the ability of HNO to reduce the iron(III) center.[20] During experiments examining the possible generation of HNO from *trans*-$[Ru^{II}(NO^+)(NH_3)_4(P(OEt)_3)]^{3+}$, myoglobin was used as an HNO trap.[1] A significant change was observed in the myoglobin spectrum simply by mixing the above ruthenium nitrosyl and the myoglobin.

In order to verify the possibility that iron(III) nitrosylation occurs without requiring a nitrosonium activation pathway, we investigated the NO transfer reaction between the iron(III) species $[Fe^{III}(H_2O)TPPS]$, metmyoglobin, and hemoglobin and ruthenium nitrosyl complexes *trans*-$[Ru^{II}(NO^+)(NH_3)_4(L)]^{3+}$. We interpret this reaction as an unprecedented example of an inner-sphere electron transfer process through an NO bridge.

EXPERIMENTAL SECTION

Reagents and Synthesis. Ruthenium(III) chloride hydrate (Strem Chemicals), hydrazine monohydrate 99% (Sigma-Aldrich), hydrochloric acid 37% (Aldrich), trifluoroacetic acid 99% (Sigma-Aldrich), zinc ≥99.9% (Aldrich) and mercury 99.99% (Sigma-Aldrich) to prepare zinc amalgam, sodium nitrite 99% (Sigma-Aldrich),

Received: January 17, 2014
Published: April 16, 2014

   dx.doi.org/10.1021/ic500122b | *Inorg. Chem.* 2014, 53, 4475−4481

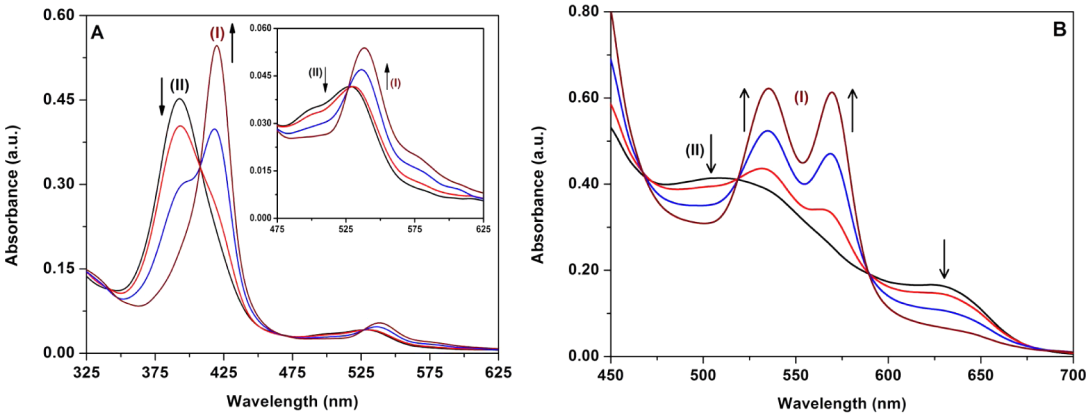

Figure 1. Spectral changes during the reaction of iron(III) species with the *trans*-$[Ru^{II}(NO^+)(NH_3)_4(P(OEt)_3)]^{3+}$ ion in aqueous solution. (A) C_{Ru} = 6.0 × 10^{-5} mol L^{-1}; $C_{[Fe^{III}TPPS]}$ = 3.0 × 10^{-6} mol L^{-1}; (B) C_{Ru} = 8.0 × 10^{-4} mol L^{-1}; C_{metMb} = 4.0 × 10^{-5} mol L^{-1}. T = 25.0 ± 0.1 °C.

ammonium hexafluorophosphate 99% (Strem Chemicals), imidazole 99% (Aldrich), isonicotinamide 99% (Aldrich), nicotinamide 98% (Sigma), and diethyl phosphite 98% (Aldrich) were used as received. Trimethyl and triethyl phosphite 98% (Sigma-Aldrich) were treated with metallic sodium, distilled under vacuum, and ampuled (1.0 mL) under an argon atmosphere. The reagents iron sulfate heptahydrate (Merck), 4,4′,4″,4‴-(porphine-5,10,15,20-tetrayl)tetrakis-(benzenesulfonic acid) tetrasodium salt hydrate (TPPS, Aldrich), Dowex 50WX8-200 (Sigma-Aldrich), and acetone and methanol HPLC grade (Panreac) were used as received. The complexes *trans*-$[Ru^{II}(NO^+)(NH_3)_4(L)](X)_3$ and its synthetic precursors were synthesized as described before.[21−26] The $[Fe^{III}(Cl)(TPPS)]$ synthetic procedure followed the literature.[27]

Experimental Procedures. All solutions were prepared using high-purity water (Milli-Q system, Bedford, MA, USA). Solutions of trifluoroacetic acid (pH = 4.0; μ = 0.1 mol L^{-1} CF_3COOH/CF_3COONa) were used in all experiments, unless otherwise mentioned. The temperature was always kept at 25.0 ± 0.1 °C. All manipulations were performed in an inert atmosphere using high-purity argon or using a Schlenk line by the freeze−pump−thaw method.[27] Argon was purified by passing it through a washing flask containing Cr(II) in acidic medium and then in a second vessel containing concentrated sulfuric acid.[28] After this treatment, the residual oxygen in the gas was lower than 10 ppb.[28] Myoglobin from equine skeletal muscle (Sigma) and human hemoglobin (Sigma) were purified by passing its solutions through a glass column (1.0 × 10.0 cm) filled with Sephadex G-25 (Sigma) as solid phase.[29] The previously mentioned trifluoroacetic acid solutions were used as eluent. The protein concentration in the solution was determined by UV−vis spectroscopy (myoglobin: λ = 502 nm, ε = 9.5 × 10^3 L mol^{-1} cm^{-1};[30] hemoglobin: λ = 530 nm, ε = 1.0 × 10^4 L mol^{-1} cm^{-1} [31]). Solutions of $[Fe^{III}(Cl)TPPS]$ were prepared by dissolving the required amount of solid in the previously mentioned trifluoroacetic acid solution, and the concentration was checked using the UV−vis spectrum (λ = 392 nm; ε = 1.55 × 10^5 L mol^{-1} cm^{-1}).[32] Electronic spectra were obtained on a Hitachi U3501 spectrophotometer (Tokyo, Japan) or on a Thermo Multiskan GO (Vantaa, Finland) spectrophotometer using a 1.00 cm path length quartz cell. For the measurements in an inert atmosphere, a high-vacuum glass stopcock was adapted to the cuvette. Electron paramagnetic resonance spectra were obtained using a Bruker EMX Plus spectrometer (Rheinstetten, Germany) coupled with a standard or cylindrical cavity operating in the X-band. The reaction progress was followed by electron paramagnetic resonance spectroscopy (EPR) by transferring aliquots of a stock aqueous solution where the reaction was taking place directly in a previously deaerated 4 mm quartz EPR tube (Wilmad Labglass, USA). The spectra were recorded at −196 °C ($N_{2(l)}$) or −263 °C ($He_{(l)}$). For field calibration, a capillary tube containing DPPH• was used. Cyclic voltammetry (CV) and differential pulse voltammetry (DPV) were performed in a PAR 264A potentiostat/galvanostat (Princeton, USA). A three-electrode system—a glassy carbon or a PAR static mercury drop electrode (SMDE), model 303A, as working electrodes, platinum plate as auxiliary electrode, and a saturated calomel electrode as reference—was used. All potentials reported are converted to the normal hydrogen electrode (NHE). The NO detection in solution was carried out by an electrochemical apparatus from Innovative Instruments, model inNO-T, coupled with an amino 700 electrode (maximum electrode response: 200pA/nmol of NO). The detection limit determined in the experimental conditions utilized was 5.0 × 10^{-7} mol L^{-1} of NO.

Kinetics Treatment. The kinetic analysis was performed using a reaction model based on a two-step reaction, described in detail in the Supporting Information. The absorbance curves were normalized to simplify the fitting procedure.

DFT Calculations. Molecular optimizations by DFT[33] were carried out using a Gaussian 03 package[34] with the B3LYP exchange−correlation function.[35,36] The Density Gauss Double-Zeta Valence Polarized basis set[37−39] (DGDZVP) was used for all atoms. All calculations were performed using the IEPCM solvation method.[40−42] The transition-state structures were optimized using the QST3 without freezing the molecular coordinates.

RESULTS

Product and Stoichiometry Analysis: Reactions of *trans*-$[Ru^{II}(NO^+)(NH_3)_4(L)]^{3+}$ with $[Fe^{III}(Cl)TPPS]$ and Metmyoglobin. The reaction of *trans*-$[Ru^{II}(NO^+)(NH_3)_4(L)]^{3+}$ with $[Fe^{III}(Cl)TPPS]$ and metmyoglobin referred to herein as $[Fe^{III}TPPS]$ and metMb, respectively, was followed using UV−vis spectroscopy. When L = ImN, IsN, Nic, and $P(OH)(OEt)_2$, no reaction was observed even with a large excess (150-fold excess over the iron(III) species) of the ruthenium complexes. However, when L = $P(OEt)_3$ and $P(OMe)_3$, the reaction occurred immediately. Figure 1A and B show the progress of the reactions of *trans*-$[Ru^{II}(NO^+)(NH_3)_4(P(OEt)_3)]^{3+}$ with $[Fe^{III}TPPS]$ and with metMb in aqueous solution. During the course of the reaction new bands were observed at 420/538 nm for $[Fe^{III}TPPS]$ (Figure 1A (I)), with isosbestic points at 407, 460, and 529 nm. For metMb, the new bands were observed at 535/570 nm (Figure 1B (I)) with isosbestic points at 482, 518, and 598 nm. The band maxima (420, 533 and 535, 570 nm) correspond to the iron(II) nitrosyl $\{Fe^{II}(NO^+)\}^6$ formation.[32] The same behavior was observed for the reaction between human hemoglobin and *trans*-$[Ru^{II}(NO^+)(NH_3)_4(P(OEt)_3)]^{3+}$ (Supporting Information, Figure S1). Also, following the reaction in the presence of selective NO electrode, it was not possible to observe the presence of free NO in the solution.

dx.doi.org/10.1021/ic500122b | Inorg. Chem. 2014, 53, 4475−4481

The reaction was also followed by electron paramagnetic resonance spectroscopy for detecting the formation of a paramagnetic species with g = 2.42, as exemplified in Figure 2, whose spectrum matches with the one previously reported

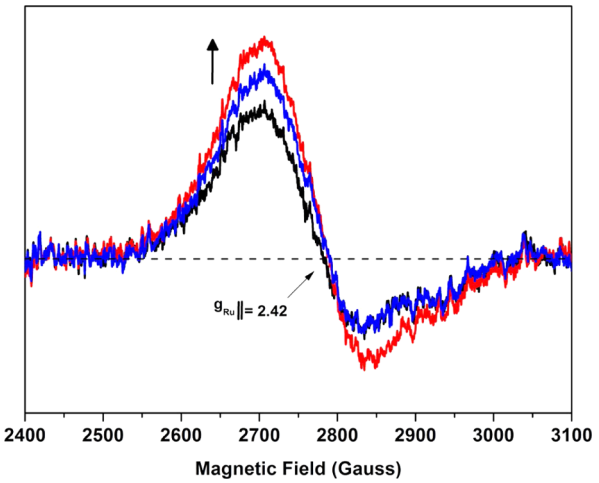

Figure 2. EPR spectra showing *trans*-$[Ru^{III}(H_2O)(NH_3)_4(P(OEt)_3)]^{3+}$ formation during the reaction between *trans*-$[Ru^{II}(NO^+)(NH_3)_4(P(OEt)_3)]^{3+}$ and $[Fe^{III}TPPS]$. C_{Ru} = 1.5 × 10^{-3} mol L^{-1}; $C_{[Fe^{III}TPPS]}$ = 7.5 × 10^{-5} mol L^{-1}; T = −196 °C. Microwave frequency: 9.4559 GHz. The $g_\perp$ = 1.72 was not observed by its intrinsic small intensity in the EPR spectrum and for the small concentration of Ru(III) formed during the reaction.

for *trans*-$[Ru^{III}(H_2O)(NH_3)_4(P(OEt)_3)]^{3+}$.[43] Since the concentration of Ru(III) formed is in the range 10^{-5} mol L^{-1}, the signal−noise relation of the spectra is small, with the identification of the $g_\perp$ = 1.72 becoming impracticable. Thus, to confirm the formation of the Ru(III) species, CV experiments were conducted and an anodic peak at $E^{0\prime}_{Ru^{III}/Ru^{II}}$ = 0.70 V[24] was observed, matching with the formation of the *trans*-$[Ru^{III}(H_2O)(NH_3)_4(P(OEt)_3)]^{3+}$ complex (Figure S2, Supporting Information). A similar behavior was observed when L = $P(OMe)_3$.

The quantification of the $[Fe^{II}(NO^+)]$ species ($[Fe^{II}(NO^+)$-TPPS]: λ_{max} = 420 nm/ε = 2.56 × 10^5 L mol^{-1} cm^{-1}; $[MbFe^{II}(NO^+)]$: λ_{max} = 536 nm/ε = 9.0 × 10^3 L mol^{-1} cm^{-1})[32] and the quantitative conversion of *trans*-$[Ru^{II}(NO^+)(NH_3)_4(P(OEt)_3)]^{3+}$ into *trans*-$[Ru^{III}(H_2O)(NH_3)_4(P(OEt)_3)]^{3+}$ strongly suggest that the following overall reaction has occurred:

$$\textit{trans}\text{-}[Ru^{II}(NO^+)(NH_3)_4(P(OR)_3)]^{3+} + [Fe^{III}(L)] \rightarrow \textit{trans}\text{-}[Ru^{III}(H_2O)(NH_3)_4(P(OR)_3)]^{3+} + [Fe^{II}(NO^+)] \quad (5)$$

Kinetic Analysis, Proposed Mechanism, and Thermodynamics. A sigmoidal curve was obtained by plotting absorbance corresponding to the formation of the $\{Fe^{II}(NO^+)\}^6$ species versus time, suggesting the formation of intermediate species,[44,45] Figure 3.

Based on the absorbance profile above, and taking in account the reported data in the literature for binuclear compounds with a bridging NO ligand,[13−19] the following reaction scheme was proposed (eqs 6 and 7):

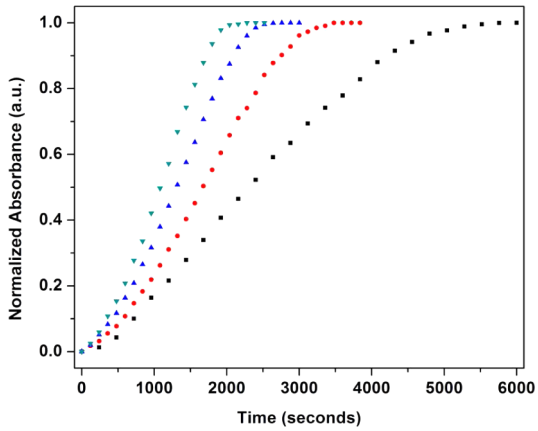

Figure 3. Time dependency absorption profile for the reaction of $[Fe^{III}TPPS]$ with the *trans*-$[Ru^{II}(NO^+)(NH_3)_4(P(OEt)_3)]^{3+}$ ion in aqueous solution. $C_{[Fe^{III}TPPS]}$ = 3.0 × 10^{-6} mol L^{-1}. Ratio Fe:Ru (■) 1:10; (●) 1:20; (▲) 1:30; (▼) 1:40. Curves correspond to the formation of $[Fe^{II}(NO^+)TPPS]$ at λ = 420 nm.

$$\textit{trans}\text{-}[Ru^{II}(NO^+)(NH_3)_4(P(OR)_3)]^{3+} + [Fe^{III}(L)] \xrightarrow{k_1} [(P(OR)_3)(NH_3)_4Ru^{II}(\mu\text{-}NO^+)Fe^{III}(L)]^n \quad (6)$$

$$[(P(OR)_3)(NH_3)_4Ru^{II}(\mu\text{-}NO^+)Fe^{III}(L)]^n \xrightarrow{k_2} \textit{trans}\text{-}[Ru^{III}(H_2O)(NH_3)_4(P(OR)_3)]^{3+} + [Fe^{III}(NO^+)] \quad (7)$$

Using the expressions described in the Supporting Information, the specific rate constants (k_1, k_2) listed in Table 1 were calculated.

Table 1. Calculated Specific Rate Constants[a] for the Reaction between *trans*-$[Ru^{II}(NO^+)(NH_3)_4(L)]^{3+}$ and Iron(III) Species

L[b]	$[Fe^{III}(L)]$	k_1 (L mol^{-1} s^{-1})	k_2 (s^{-1})
$P(OMe)_3$	TPPS	7.7 ± 0.5	(2.7 ± 0.1) × 10^{-3}
	metMb	1.1 ± 0.1	(5.3 ± 0.10 × 10^{-3}
$P(OEt)_3$	TPPS	2.8 ± 0.1	(2.4 ± 0.4) × 10^{-3}
	metMb	2.1 ± 0.1	(11.4 ± 0.5) × 10^{-3}
	Hb	2.4 ± 0.2	(8.5 ± 0.5) × 10^{-3}

[a] T = 25.0 ± 0.1 °C, pH = 4.0 (CF_3COOH/CF_3COONa; μ = 0.1 mol L^{-1}). [b] For L = $P(OH)(OEt)_2$, ImN, IsN, and Nic no reaction was observed.

The thermodynamic activation parameters of the reaction between $[Fe^{III}TPPS]$ and *trans*-$[Ru^{II}(NO^+)(NH_3)_4(P(OEt)_3)]^{3+}$ were calculated using the Eyring equation (Tables S1 and S2 and Figure S3, Supporting Information). For the first (k_1) and second (k_2) reaction steps the activation parameter values found were respectively $\Delta H^{\ddagger}$ = 104.9/70.3 kJ mol^{-1}, $\Delta S^{\ddagger}$ = 144.8/−57.7 J mol^{-1} K^{-1}, and $\Delta G^{\ddagger}$ = 61.1/87.4 kJ mol^{-1}.

Identification of the Binuclear Intermediate. Following the reaction between $[Fe^{III}TPPS]$ and *trans*-$[Ru^{II}(NO^+)(NH_3)_4(P(OEt)_3)]^{3+}$ by electrochemical techniques (CV and DPV), two new cathodic waves, E_{cp1} = −0.47 V and E_{cp2} = −0.35 V, Figure 4A, appeared in the voltammetric spectra during the course of the reaction. It is important to emphasize that theses peaks were not present at the beginning of the

dx.doi.org/10.1021/ic500122b | Inorg. Chem. 2014, 53, 4475−4481

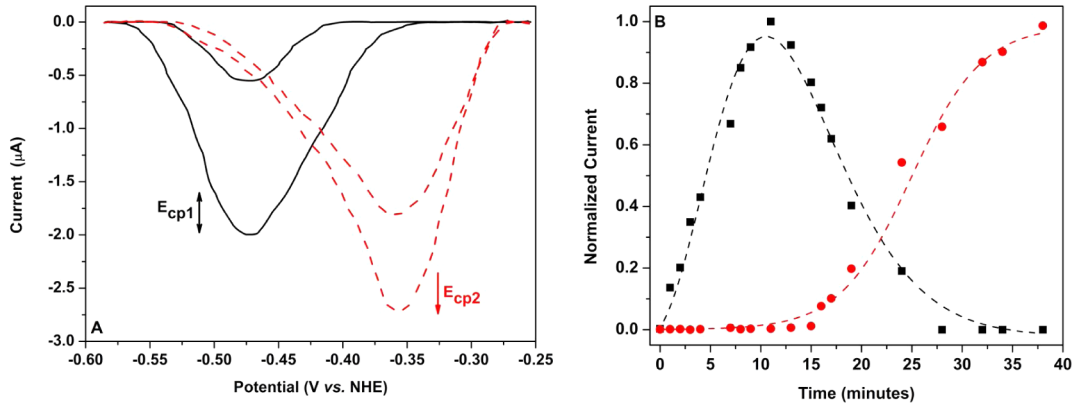

Figure 4. (A) DPV curves obtained using the SMDE electrode of the reaction between $[Fe^{III}TPPS]$ and *trans*-$[Ru^{II}(NO^+)(NH_3)_4(P(OEt)_3)]^{3+}$. Solid line (black): binuclear formation and decay; dashed line (red): product formation. $C_{Ru} = 7.15 \times 10^{-4}$ mol L^{-1}; $C_{[Fe^{III}TPPS]} = 7.15 \times 10^{-5}$ mol L^{-1}; $T = 25.0 \pm 0.1$ °C. (B) Plot of normalized current versus time using the DPV data.

reaction. The current−time profile for the E_{cp1} showed a behavior compatible with the one exhibited for the formation and decay of the proposed binuclear species (Figure 4B, black line). Also, the electrochemical process (E_{cp1}) was shown to be irreversible. The potential window in which these electrochemical processes were observed is distant from the redox couples for $[Fe^{III}(H_2O)TPPS]$ ($E^{0\prime}_{Fe^{III}/Fe^{II}} = 0.014$ V),[27] *trans*-$[Ru^{II}(NO^+)(NH_3)_4(P(OEt)_3)]^{3+/2+}$ ($E^{0\prime}_{NO^+/NO^0} = 0.11$ V),[2] or *trans*-$[Ru^{III}(H_2O)(NH_3)_4(P(OEt)_3)]^{3+/2+}$ ($E^{0\prime}_{Ru^{III}/Ru^{II}} = 0.70$ V).[24] Therefore, the E_{cp1} process was tentatively interpreted as one-electron reduction of the heterobinuclear complex, eq 8.

$$[(P(OR)_3)(NH_3)_4Ru^{II}(\mu\text{-}NO)Fe^{III}(L)]^n \xrightarrow{1e^-} [(P(OR)_3)(NH_3)_4Ru^{II}(\mu\text{-}NO)Fe^{III}(L)]^{(n-1)} \quad (8)$$

By plotting the peak current of peak E_{cp2} versus time (Figure 4 B, red curve) a sigmoidal behavior was observed for the product formation, which is similar to the one shown in Figure 3. As reported by Meyer,[27] the reduction potential for the $[Fe^{II}(NO^0)TPPS]^{4-}/[Fe^{II}(NO^-)TPPS]^{5-}$ couple is $E^{0\prime} = -0.38$ V. Since different experimental conditions could probably account for the 0.030 V difference between the values observed here ($E^{0\prime} = -0.35$ V) and the one reported in the literature, the peaks (III) and (IV) were attributed to the $[Fe^{II}(NO^0)TPPS]^{4-}/[Fe^{II}(NO^-)TPPS]^{5-}$ electrochemical process. The formation of $[Fe^{II}(NO^+)TPPS]$ was confirmed by UV−vis, providing additional support to the above assertion.

The identification of the intermediate by its UV−vis spectrum was also attempted, but without conclusive results. By trying to extract the spectrum for any intermediate formed during the time scale of the reaction, taking into account both reagents and products, it was still not possible to observe any new band in the resulting spectrum. Using TD-DFT for the optimized structure of the intermediate it was observed that the proposed intermediate would exhibit an absorption band at UV, but with a molar absorptivity compared with the iron(III) species. These overlapping bands would be coherent with the nonobservation of intermediate species when following the reaction by absorption spectroscopy.

The formation of a possible binuclear complex was also investigated using DFT calculations. The structure of the intermediate was optimized with NO as a bridging ligand. Taking into account the composition of the molecular orbitals presented in Table S3 (Supporting Information), it can be observed that the HOMO and HOMO−1 orbitals are centered in the porphyrin ring, while HOMO−2 is concentrated predominantly on the NO ligand (46%). Table S3 also shows that the composition of HOMO−12 (Fe: 11%; NO: 2%; Ru: 51%; TPPS: 5%; NH_3: 2%; $P(OEt)_3$: 29%) is delocalized along the [Ru−(μNO)−Fe] axis, representing a ligand interaction, coherently with the formation of the binuclear species.

With regard to LUMO and LUMO+1 orbitals, the main contribution of their composition is centered in the NO ligand (17% and 80%, respectively), which predicts that reduction of the binuclear species, as observed in Figure 4, would probably occur in this fragment. This observation reinforces the hypothesis that the E_{CP1} peak observed in the DPV corresponds to the electrochemical process presented in eq 8. Also, the slight energy difference between the LUMO and LUMO+1 orbitals (0.9 kcal mol^{-1}) indicates they are nearly degenerate. Figure S4 (Supporting Information) shows the optimized structure for the binuclear complex and the density plots of the orbitals discussed above.

DISCUSSION

Since the complexes *trans*-$[Ru^{II}(NO^+)(NH_3)_4(L)]^{n+}$ only liberate NO in solution after a one-electron reduction, with specific rate constants ranging from 2.5×10^{-2} (L = IsN) to 0.98 s^{-1} (L= $P(OEt)_3$), the spontaneous dissociation of NO is unlikely to occur due to the nitrosonium characteristic of the NO ligand in these complexes.[2] Therefore, taking into account the experimental data of Table 1 and the accumulated kinetic data of the ruthenium and iron species, the reaction mechanism described by eqs 1 and 2 is unlikely to occur. Thus, it is quite reasonable to assume that the reaction observed between the ruthenium nitrosyl complexes and iron(III) species takes place through the mechanism described by eqs 3 and 4.

The nature of the ligand *trans* positioned to NO^+ in the ruthenium nitrosyl complexes proved to be important in the reactivity of these complexes. As observed, the reaction occurs only when the phosphorus esters $P(OMe)_3$ and $P(OEt)_3$, but not $P(OH)(OEt)_2$, are present in the coordination sphere. These phosphorus ligands exhibit the highest π-acidity among all the other ligands dealt with in this work.[2,48] The higher the π-acidity of the NO *trans* ligand, the more electrophilic is the NO ligand (observed by $\nu(NO^+)$ and $E^{0\prime}_{NO^+/NO^0}$ values in Table S4), and therefore, the easier it is for the reaction to occur.

dx.doi.org/10.1021/ic500122b | Inorg. Chem. 2014, 53, 4475−4481

The values of k_1 and k_2 for the reaction between the iron(III) species and ruthenium nitrosyls are similar, even when considering the structural differences between the heme proteins and the [Fe^{III}TPPS] redox potential values for these iron(III) species are close to each other (14, 38, and 72 mV vs NHE, for [$Fe^{III}(H_2O)$TPPS], Hb, and metMb, respectively).[27,31] Also, we observe a good correlation of the k_1 and k_2 values with $E^{0\prime}_{Fe^{III}/Fe^{II}}$ values (Supporting Information, Figure S5). Since the values of k_1 and k_2 for the same nitrosyl complex do not differ significantly with the nature of the iron(III) species, the steric hindrance of the iron(III) center does not seem to be the main factor contributing to the values of the rate constants.

The changes in the electronic spectra of the [$Fe^{III}(H_2O)$-TPPS] by mixing solutions of *trans*-[$Ru^{II}(NO^+)(NH_3)_4(L)]^{3+}$ and [$Fe^{III}(H_2O)$TPPS] indicate that electron transfer occurs between the ruthenium and iron centers. However, this observation does not provide any information about the association between these two ions in the absence of electron transfer. This information was obtained by performing experiments using differential pulse voltammetry and conductometry. The voltammograms for the reduction of the nitrosyl ligand in the complexes *trans*-[$Ru^{II}(NO^+)(NH_3)_4(L)]^{3+}$ (L = ImN, IsN, Nic, and $P(OH)(OEt)_2$) were found to be unchanged by the addition of [$Fe^{III}(H_2O)$TPPS] to the solution. Thus, no shift is observed in $E_{(NO^+/NO^0)}$ and no increase observed in the half-wave values ($W_{1/2}$). This information strongly suggests that for these complexes there is no interaction at the nitrosyl ligand in the presence of the iron compound. This is not the case for L = $P(OEt)_3$ and $P(OMe)_3$ as previously mentioned. Conductometric measurements provide additional support for this. Except for L = $P(OEt)_3$ and $P(OMe)_3$, no changes were observed in the solution conductance, for a 1 h period, when solutions of *trans*-[$Ru^{II}(NO^+)(NH_3)_4(L)]^{3+}$ and [$Fe^{III}(H_2O)$TPPS] were mixed. When L = $P(OEt)_3$ and $P(OMe)_3$, there is a substantial conductance decrease within the first 10 min, after which the conductance increases. This behavior is in agreement with that expected, according to eqs 6 and 7.

The absorbance versus time profile strongly suggests the formation of a single intermediate species,[44,45] supporting the reactions represented in eq 6 and 7. In the second step, the binuclear species dissociates, yielding the products in a straightforward reaction. No evidence of rate saturation was observed in plots of k_{obs} versus C_{Ru} in the concentration range studied. At iron concentrations higher than 1.0×10^{-4} mol L^{-1} and a 10-fold excess of ruthenium, a dark brown precipitate is formed in a low yield (<5%). The characterization of this solid using elemental analysis ICP-OS was inconclusive. However, an EPR spectrum (Figure S6, Supporting Information) of this solid at −263 °C showed the presence of two distinct iron paramagnetic species. The g = 5.8 species is attributed to high-spin Fe(III), probably [$Fe^{III}(H_2O)$TPPS], and the g = 2.03 species is described in the literature and attributed to [$Fe^{II}(NO^{\bullet})$TPPS] species.[46]

In the first step the formation of the binuclear species, with the specific rate constants (k_1) reported in Table 1, arises from the interaction between the electron in the d_{z^2} orbital of the [Fe^{III}(TPPS)]$^{3-}$ and the empty pπ^* orbitals of the [$Ru^{II}(NO^+)]^{3+}$ complex, passing through the first transition state (TS#1). This suggests an electrophilic attack of an Fe(III) species on the coordinated NO^+ in the Ru(II) complex. At first sight it seems unlikely that the nucleophile in this reaction is the Fe(III), which is generally considered an electron-poor species. However, in the models studied herein, the Fe(III) species are high spin.[47] Thus, there is one unpaired electron in the d_{z^2} orbital, which by the DFT calculation of the species [$Fe^{III}(H_2O)$TPPS] is the HOMO orbital of the molecule. Also DFT calculations for the complex *trans*-[$Ru^{II}(NO^+)(NH_3)_4$(P-$(OEt)_3)]^{3+}$ indicate that the LUMO and LUMO+1 orbitals, both degenerate, are concentrated predominantly on the nitrosonium ligand, thus suggesting a possible nucleophilic attack of the Fe(III) on the nitrosonium ligand. The electron transfer occurs after the formation of the intermediate, leading to a second species, still with NO as bridging ligand, but with the oxidized ruthenium and reduced iron centers. After the electron is transferred, the bond between ruthenium and NO begins to break, yielding [$Fe^{II}(NO^+)$(TPPS)]$^{3-}$ and [$Ru^{III}(H_2O)]^{3+}$ as products, with the specific rate constants (k_2) as shown in Table 1.

The activation parameter values found indicate that the reaction is exergonic. The values found for $\Delta H^{\ddagger}$ and $\Delta G^{\ddagger}$ are coherent with other bimolecular reactions.[46,48] Previously studies[49,50] involving the reaction between NO and [Fe^{III}(TPPS)] and metMb indicate that the water dissociation is the first step for the reaction between iron(III) species and NO. Ford and van Eldik described activation parameters for these reactions: 70 ± 3/71 ± 2 kJ mol^{-1} and 100 ± 4/82 ± 7 J mol^{-1} K^{-1} for $\Delta H^{\ddagger}$ and $\Delta S^{\ddagger}$ for [Fe^{III}(TPPS)] and metMb, respectively. These values are in reasonable agreement with the values obtained in this work and would suggest that the NO transfer, as an example of the other reported reactions with iron(III) species described in the literature,[49,50] is controlled by the water dissociation step.

It is interesting to observe that the value of $\Delta S^{\ddagger}$ is positive for the formation of the binuclear species and negative for the intermediate broken. This behavior is not expected, but can be explained, in addition to the possible water dissociative pathway, by the large solvation changes during the reactions, mostly in the transition-state structures.[44,45]

Taking in account the reactants, the products, and the postulated intermediate (optimized by DFT calculations) some interesting points can be inferred. First, the value of k_{et} between the two metal centers tends to be slow, since there is an orbital symmetry impediment for the electron transfer. The [Ru^{II}–NO^+] bond consists of a σ component involving the Ru d_{z^2} orbital and NO ligand and a π component involving the orbitals Ru d_{zy} and d_{zx} and the NO pπ^* orbitals. In the binuclear species, the bond between Ru, Fe, and NO is formed by the interaction of the pπ^* orbital of [$Ru^{II}NO^+$] fragment with the d_{z^2} orbital of Fe, which has σ symmetry. With this perspective, the oxidation of the Ru(II) center will occur using the d_{zy} or d_{zx} orbitals, which interact with both the NO^+ and iron species. In short, the electron transfer between the two metal centers will occur through the ruthenium π-symmetry orbitals and iron σ orbital. The symmetry difference makes the electron transfer a slow process. DFT calculations show a delocalized bonding orbital (HOMO−12) connecting the Ru, Fe, and NO^+ centers, with a ligand characteristic that could probably be the one involved in the electron transfer. Figure S4 (Supporting Information) shows the contour surface of HOMO−12 for the binuclear species.

After the electron transfer, the bond-breaking rate constant between Ru(III) and NO^+ is 2.4×10^{-3} s^{-1} for the reaction between *trans*-[$Ru^{II}(NO^+)(NH_3)_4(P(OEt)_3)]^{3+}$ and [Fe^{III}(TPPS)]$^{3-}$, Table 1. There are few examples of water

dx.doi.org/10.1021/ic500122b | Inorg. Chem. 2014, 53, 4475−4481

substitution in ruthenium(III) ammine complexes with a phosphorus ligand in one of the axial positions, being limited to the specific rate constant for substitution of isonicotinamide by water in *trans*-$[Ru^{III}(IsN)(NH_3)_4(P(OEt)_3)]^{3+}$, calculated as 5.0×10^{-5} s^{-1}. Comparing the rate constants the specific rate constant is found to be 48-fold higher for water substitution in the binuclear complex. One possible explanation for the higher specific rate constant for aquation of the binuclear complex is the presence of Fe(II) bonded to the NO^+, since the bond between $[Fe^{II}(NO^+)]$ is stronger than $[Ru^{III}(NO^+)]$, due to the presence of back-bonding in the iron nitrosyl complex.

The electrochemical experiments and the DFT calculations for the title reactions strongly suggest the formation of a binuclear species, as described in eqs 6 and 7. Therefore, the electroactive species at $E_{cp1} = -0.47$ V was tentatively attributed to the bridged nitrosonium ligand reduction, as described in eq 8. This is the site were the reduction would probably occur. The NO reduction in the binuclear complex could be coherently shifted to more negative potentials with respect to that observed in the complex *trans*-$[Ru^{II}(NO^+)(NH_3)_4(P(OR)_3)]^{3+}$ owing to the electron density delocalization along the [Ru−(μNO)−Fe] bridge.

The NO transfer reactions of manganese, iron, and chromium complexes have already been reported in the literature.[13−19] However, the results described herein are the first examples of this reaction with ruthenium nitrosyls.

The possibility of direct NO transfer to biological desired targets demonstrated by the title complexes can be an alternative pathway for NO delivery chemistry. Most of the NO donors reported in the literature liberate NO, spontaneously or activated, in solution, and then the liberated NO reacts with the biological targets. However, due to the reactivity of NO, this species can react readily with other molecules, decreasing the NO biological activity or leading to undesired biological effects. The direct NO transfer discussed here may circumvent these inconveniences since no NO is liberated in the medium until the NO carrier hits the target, providing an alternative pathway to form iron or thiol nitrosyl complexes in biological systems. Also, not only myoglobin but also hemoglobin reacts with the nitrosyl complexes, showing that this reaction may be extended to other Fe(III)-containing proteins.

CONCLUSION

On the basis of the analysis of reaction products and kinetic data the reactions of ruthenium nitrosyls and selected iron(III) species were found to differ from other nitric oxide transfer reactions previously reported. The nitrosonium ligand on the ruthenium moiety acts as an electron transfer bridge between the two metal centers, providing an unprecedented example of an inner-sphere electron transfer process through an NO bridge. The relatively stable intermediate species [Ru(μ-NO)Fe] was predicted by DFT calculations and detected by DPV, from which the formation and decay of this species was monitored. The calculated rate constants for the sequence of reactions are in agreement with other reactions involving ruthenium tetraammine complexes. The reaction proposed herein may be one alternative pathway for the nitrosylation of iron-containing proteins and consequently its modification *in vivo* by ruthenium nitrosyl complexes. Furthermore, it could become relevant in situations where NO dissociation occurs slowly.

ASSOCIATED CONTENT

Supporting Information

This material is available free of charge via the Internet at http://pubs.acs.org.

AUTHOR INFORMATION

Corresponding Author

*E-mail: douglas@iqsc.usp.br.

Notes

The authors declare no competing financial interest.

ACKNOWLEDGMENTS

The authors acknowledge FAPESP and CNPq (grant numbers 2012/2365-4 and 475631/2011-0, respectively) for the financial support. The authors are also indebted to A.B.P. Lever (York University), Bruce R. King (University of Georgia), and Edward I. Solomon (Stanford University) for helpful discussions during the preparation of the manuscript.

DEDICATION

Dedicated to the memory of Professor Edson Rodrigues.

REFERENCES

(1) Metzker, G.; Stefaneli, E. V.; Pereira, J. C. M.; Lima, F. C. A.; Silva, S. C.; Franco, D. W. *Inorg. Chim. Acta* **2013**, *394*, 765−769.
(2) Tfouni, E.; Krieger, M.; McGarvey, B. R.; Franco, D. W. *Coord. Chem. Rev.* **2003**, *236*, 57−69.
(3) Ford, P. C.; Bourassa, J.; Miranda, K. M.; Lee, B.; Lorkovic, I.; Boggs, S.; Kudo, S.; Laverman, L. *Coord. Chem. Rev.* **1998**, *171*, 185−202.
(4) Serli, B.; Zangrando, E.; Gianferrara, T.; Yellowlees, L.; Alessio, E. *Coord. Chem. Rev.* **2003**, *245*, 73−83.
(5) Clarke, M. J. *Coord. Chem. Rev.* **2003**, *236*, 207−231.
(6) Tfouni, E.; Doro, F. G.; Figueiredo, L. E.; Pereira, J. C. M.; Metzker, G.; Franco, D. W. *Curr. Med. Chem.* **2010**, *17*, 3643−3657.
(7) DuMond, J. F.; King, S. B. *Antioxid. Redox Signaling* **2011**, *14*, 1637−1648.
(8) Tfouni, E.; Truzzi, D. R.; Tavares, A.; Gomes, A. J.; Figueiredo, L. E.; Franco, D. W. *Nitric Oxide* **2012**, *26*, 38−53.
(9) Thomas, D. D.; Miranda, K. M.; Colton, C. A.; Citrin, D.; Espey, M. G.; Wink, D. A. *Antioxid. Redox Signaling* **2003**, *5*, 307−317.
(10) Ballou, D. P.; Zhao, Y.; Brandish, P. E.; Marletta, M. A. *Proc. Natl. Acad. Sci. U.S.A.* **2002**, *99*, 12097−12101.
(11) Marozkina, N. V.; Gaston, B. *Biochim. Biophys. Acta* **2012**, *1820*, 722−729.
(12) Fukuto, J. M.; Cisneros, C. J.; Kinkade, R. L. *J. Inorg. Biochem.* **2013**, *118*, 201−208.
(13) Caulton, K. G. *J. Am. Chem. Soc.* **1973**, *95*, 4076−4077.
(14) Ungermann, C. B.; Caulton, K. G. *J. Am. Chem. Soc.* **1976**, *98*, 3862−3868.
(15) Doyle, M. P.; Van Doornik, F. J.; Funckes, C. L. *Inorg. Chim. Acta* **1980**, *46*, 111−113.
(16) Doyle, M. P.; Pickering, R. A.; Dykstra, R. L.; Cook, B. R. *J. Am. Chem. Soc.* **1982**, *104*, 3392−3397.
(17) Wade, R. S.; Castro, C. E. *Chem. Res. Toxicol.* **1990**, *3*, 289−289.
(18) Mu, X. H.; Kadish, K. M. *Inorg. Chem.* **1990**, *29*, 1031−1036.
(19) Franz, K. J.; Lippard, S. J. *Inorg. Chem.* **2000**, *39*, 3722−3723.
(20) Bazylinsk, D. A.; Hollocher, T. C. *J. Am. Chem. Soc.* **1985**, *107*, 7982−7986.
(21) Vogt, L. H., Jr.; Katz, J. L.; Wiberley, S. E. *Inorg. Chem.* **1965**, *4*, 1157−1163.
(22) Ford, P. C. *Coord. Chem. Rev.* **1970**, *5*, 75−99.
(23) Isied, S.; Taube, H. *Inorg. Chem.* **1974**, *13*, 1545−1551.
(24) Franco, D. W.; Taube, H. *Inorg. Chem.* **1978**, *17*, 571−578.
(25) Diamantis, A. A.; Dubrawsky, J. V. *Inorg. Chem.* **1981**, *20*, 1142−1150.

(26) Borges, S. S. S.; Davanzo, C. U.; Castellano, E. E.; Schpector, J. Z.; Silva, S. C.; Franco, D. W. *Inorg. Chem.* **1998**, *37*, 2670−2677.
(27) Barley, M. H.; Takeuchi, K. J.; Meyer, T. J. *J. Am. Chem. Soc.* **1986**, *108*, 5816−5885.
(28) Shriver, D. F.; Drezdzon, M. A. *The Manipulation of Air-Sensitive Compounds*; Wiley: New York, 1986.
(29) Espey, M. G.; Thomas, D. D.; Miranda, K. M.; Wink, D. A. *Proc. Natl. Acad. Sci. U.S.A.* **2002**, *99*, 11127−11132.
(30) Bowen, W. J. *J. Biol. Chem.* **1949**, *179*, 235−245.
(31) Antonini, E.; Brunori, M. *Hemoglobin and Myoglobin in their Reactions with Ligands*; North-Holland: Amsterdam, 1971.
(32) Hoshino, M.; Ozawa, K.; Seki, H.; Ford, P. C. *J. Am. Chem. Soc.* **1993**, *115*, 9568−9575.
(33) Kohn, W.; Sham, L. J. *Phys. Rev.* **1965**, *140*, A1133−A1138.
(34) Frisch, M. J.; Trucks, G. W.; Schlegel, H. B.; Scuseria, G. E.; Robb, M. A.; Cheeseman, J. R.; Montgomery, J. A., Jr.; Vreven, T.; Kudin, K. N.; Burant, J. C.; Millam, J. M.; Iyengar, S. S.; Tomasi, J.; Barone, V.; Mennucci, B.; Cossi, M.; Scalmani, G.; Rega, N.; Petersson, G. A.; Nakatsuji, H.; Hada, M.; Ehara, M.; Toyota, K.; Fukuda, R.; Hasegawa, J.; Ishida, M.; Nakajima, T.; Honda, Y.; Kitao, O.; Nakai, H.; Klene, M.; Li, X.; Knox, J. E.; Hratchian, H. P.; Cross, J. B.; Bakken, V.; Adamo, C.; Jaramillo, J.; Gomperts, R.; Stratmann, R. E.; Yazyev, O.; Austin, A. J.; Cammi, R.; Pomelli, C.; Ochterski, J. W.; Ayala, P. Y.; Morokuma, K.; Voth, G. A.; Salvador, P.; Dannenberg, J. J.; Zakrzewski, V. G.; Dapprich, S.; Daniels, A. D.; Strain, M. C.; Farkas, O.; Malick, D. K.; Rabuck, A. D.; Raghavachari, K.; Foresman, J. B.; Ortiz, J. V.; Cui, Q.; Baboul, A. G.; Clifford, S.; Cioslowski, J.; Stefanov, B. B.; Liu, G.; Liashenko, A.; Piskorz, P.; Komaromi, I.; Martin, R. L.; Fox, D. J.; Keith, T.; Al-Laham, M. A.; Peng, C. Y.; Nanayakkara, A.; Challacombe, M.; Gill, P. M. W.; Johnson, B.; Chen, W.; Wong, M. W.; Gonzalez, C.; Pople, J. A. *Gaussian 03*; Gaussian Inc.: Wallingford, CT, 2004.
(35) Lee, C.; Yang, W.; Parr, R. G. *Phys. Rev. B* **1998**, *37*, 785−799.
(36) Becke, A. D. *J. Chem. Phys.* **1993**, *98*, 5648−5652.
(37) Hay, P. J.; Wadt, W. R. *J. Chem. Phys.* **1985**, *82*, 270−283.
(38) Wadt, W. R.; Hay, P. J. *J. Chem. Phys.* **1985**, *82*, 284−298.
(39) Hay, P. J.; Wadt, W. R. *J. Chem. Phys.* **1985**, *82*, 299−310.
(40) Cances, E.; Mennucci, B.; Tomasi, J. *J. Chem. Phys.* **1997**, *107*, 3032−3041.
(41) Reed, A. E.; Weinhold, F. *J. Chem. Phys.* **1995**, *83*, 1736−1740.
(42) Reed, A. E.; Curtiss, L. A.; Weinhold, F. *Chem. Rev.* **1988**, *88*, 899−926.
(43) Rezende, N. M. S.; Martins, S. C.; Marinho, L. A.; Santos, J. A. V.; Tabak, M.; Perussi, J.; Rodrigues, E.; Franco, D. W. *Inorg. Chim. Acta* **1992**, *182*, 87−92.
(44) Logan, S. R. *Fundamentals of Chemical Kinetics*; Prentice Hall: Essex, 1996.
(45) Connors, K. A. *Chemical Kinetics: The Study of Reactions Rates in Solution*; VCH Publishers: New York, 1990.
(46) Gilbert, D. C.; Doetschman, D. C. *Chem. Phys.* **2001**, *269*, 125−135.
(47) Gandini, S. C. M.; Vidoto, E. A.; Nascimento, O. R.; Tabak, M. *J. Inorg. Biochem.* **2003**, *94*, 127−137.
(48) Toledo, J. C.; Lima Neto, B. S.; Franco, D. W. *Coord. Chem. Rev.* **2005**, *249*, 419−431.
(49) Laverman, L. E.; Hoshino, M.; Ford, P. C. *J. Am. Chem. Soc.* **1997**, *119*, 12663−12664.
(50) Laverman, L. E.; Wanat, A.; Oszajca, J.; Stochel, G.; Ford, P. C.; van Eldik, R. *J. Am. Chem. Soc.* **2001**, *123*, 285−293.